

# Measuring photon-photon interactions via photon detection

Mihai A. Macovei\*

*Max-Planck-Institut für Kernphysik, Saupfercheckweg 1, D-69117 Heidelberg, Germany*

(Dated: November 1, 2018)

The strong non-linearity plays a significant role in physics, particularly, in designing of novel quantum sources of light and matter as well as in quantum chemistry or quantum biology. In simple systems, the photon-photon interaction can be determined analytically. However, it becomes challenging to obtain it for more complex systems. Therefore, we show here how to measure strong non-linearities via allowing the sample to interact with a weakly pumped quantized leaking optical mode. We found that the detected mean-photon number versus pump-field frequency shows several peaks. Interestingly, the interval between neighbour peaks equals the photon-photon interaction potential. Furthermore, the system exhibits sub-Poissonian photon statistics, entanglement and photon switching with less than one photon. Finally, we connect our study with existing related experiments.

PACS numbers: 42.65.Pc, 03.67.Bg, 42.50.Ar, 42.50.Lc

The non-linear interactions are perhaps the most investigated fundamental problems in modern physics and related subjects. An enormous amount of novel theoretical and experimental work has been carried out in this field. Significant results regarding this issue were obtained in quantum optics [1–12], ultracold atomic gases [13–17], quantum electronics [18–27] or quantum biochemistry [28]. Particularly, strongly interacting single photons were discussed in [2] while quantum entanglement of ultraslow single photons and quantum switching were investigated in Ref. [3], respectively. Enhanced Kerr non-linearity was reported in [4–7]. Large Kerr non-linearity has possible applications in quantum non-demolition measurements and for quantum logic gates or for optical squeezing and studies of non-locality. The effect of Kerr non-linearity on the slow light propagation was discussed in [8] whereas turning light into a liquid via atomic coherence effects was studied in [9]. A procedure by which strong high-order non-linearities can be synthesized out of low-order non-linearities was proposed in [10] while the quantum dissipative chaos in the statistics of excitation numbers was investigated in [11]. Entanglement via the Kerr non-linearity in an optical fiber system was experimentally demonstrated in [12].

A number of experiments were performed emphasizing interesting non-linear phenomena in cold atomic samples [13–16] and trapped single-atom systems in optical cavities [17]. However, atomic systems are known to exhibit not so large non-linear couplings compared with the corresponding decay rates. Hence, a significant effort was devoted towards finding systems showing ultrahigh non-linearities. Remarkable, giant Kerr non-linearities were found in quantum nanosystems [18] and quantum circuit systems [19]. The non-linearities are further responsible for a number of fascinating phenomena. Bose-Einstein condensation, bistability and electromagnetic-field-induced transparency in high-density exciton systems were shown to occur in [20, 21], while polariton

quantum blockade in a photonic dot was investigated in Ref. [22]. Signatures for a classical to quantum transition of a driven non-linear nanomechanical resonator and photon-number squeezing in circuit quantum electrodynamics were studied in [23] and [24], respectively. A proposal for detecting single-phonon transitions in a single nanoelectromechanical system was discussed as well [25]. Other non-linear effects involving macroscopic systems, superconducting qubits or biochemical samples were reported in [26–28] further advancing the research in these areas.

In many of the above mentioned effects, at least some knowledge on the non-linear interactions is required. A number of simpler samples allow the non-linearity to be determined even analytically. However, it becomes difficult to obtain it for more sophisticated systems. Therefore, here, we show how to measure the third-order non-linear susceptibility  $\chi^{(3)}$  which is responsible for the boson-boson interaction potentials, for instance. We model the system as a pumped non-linear quantum oscillator. The examined sample additionally interacts with a quantized lossy field mode. The applied field is weak such that the non-linearity is not affected by the external driving. We found that in the long-time limit, the detected photons show several peaks as function of external field detuning when the photon-photon non-linearity is larger than the quantized mode damping. Remarkably, the frequency intervals between the neighbour peaks are equal with the photon-photon interaction potential allowing us to determine it. As the strength of the pumping field is increased, the observed mean photon number shows strong asymmetrical behaviors. At lower pumping intensities switching with less than one photon occurs. Moreover, the switching effect improves for even larger non-linear interactions. The photon statistics can be sub-Poissonian. These results would disappear for vanishing boson-boson interactions. Note that for particular parameters one can create an entangled single-photon state

$|\Psi_{\pm}\rangle = (|0\rangle \pm |1\rangle)/\sqrt{2}$  with a high fidelity. Here,  $|0\rangle$  and  $|1\rangle$  are the number state basis with zero and one photon, respectively. Therefore, the study is of significance for applications ranging from optical communication to quantum processing of information.

We proceed by briefly introducing the main steps of the analytical formalism involved and then rigorously describing the obtained results. The Hamiltonian characterizing the interaction of a non-linear oscillator possessing the frequency  $\omega$  with a coherent source of frequency  $\omega_L$ , in a frame rotating at  $\omega_L$ , is:

$$H = -\Delta a^\dagger a \mp \alpha a^{\dagger 2} a^2 + \epsilon(a^\dagger + a), \quad (1)$$

where  $\Delta = \omega_L - \omega$  and  $\alpha > 0$  signifies the photon-photon non-linearity ( $\alpha \propto \text{Re}[\chi^{(3)}]$ ), while  $\epsilon$  is the amplitude of the coherent driving.  $a^\dagger$  and  $a$  are the creation and the annihilation operator of the quantum oscillator, respectively, and obeying the standard bosonic commutation relations, i.e.,  $[a, a^\dagger] = 1$ , and  $[a, a] = [a^\dagger, a^\dagger] = 0$ . The  $\mp$  sign in Eq. (1) accounts for an attractive or repulsive boson-boson interaction, respectively. Actually, the Hamiltonian (1) is abundantly investigated and characterizes a wide range of processes. A formidable approach to analyze the driven damped non-linear oscillator is via the master equation. Hence, the system is described by the reduced density operator, which in the interaction picture and under the usually applicable Born-Markov and rotating-wave approximations satisfies the master equation [29, 30]:

$$\dot{\rho} = -i[H, \rho] - \kappa([a^\dagger, a\rho] + [\rho a^\dagger, a]), \quad (2)$$

where  $\kappa$  is the decay rate of the quantized optical oscillator mode and the overdot denotes differentiation with respect to time.

In order to investigate Eq. (2) in the long-time limit and for weak excitations in more details, we first shall apply the Holstein-Primakoff transformations [31], and then follow the solving procedure developed in [32] for two-level particles. We define a state  $|q\rangle$  denoting  $N - q$  spins pointing up and  $q$  spins down. The raising and lowering spin operators act on this state as follows:  $S^+|q\rangle = \sqrt{q(2s - q + 1)}|q - 1\rangle$  and  $S^-|q\rangle = \sqrt{(q + 1)(2s - q)}|q + 1\rangle$ , where  $2s$  gives the number of excitations (spins) in the system, and  $0 \leq q \leq 2s$ . The spin operators satisfy the usual commutation relations of  $\text{su}(2)$  algebra, i.e.,  $[S_z, S^\pm] = \pm S^\pm$  and  $[S^+, S^-] = 2S_z$ , where  $S_z|q\rangle = (s - q)|q\rangle$ . Taking into account these properties, one can deduce that [31]:

$$S^+ = \sqrt{2s} \sqrt{1 - \frac{a^\dagger a}{2s}}, \quad S^- = \sqrt{2s} a^\dagger \sqrt{1 - \frac{a^\dagger a}{2s}}, \\ S_z = s - a^\dagger a. \quad (3)$$

Substituting (3) in the steady-state form of Eq. (2), observing that  $S^- S^+ = 2s a^\dagger a - a^{\dagger 2} a^2$ , and assuming lower

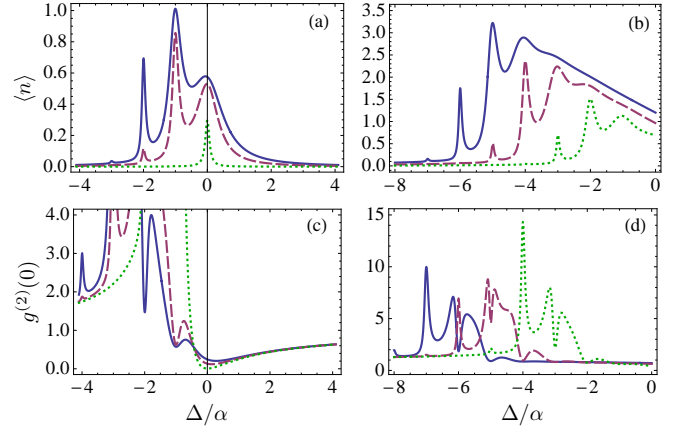


FIG. 1: (color online) The mean photon number  $\langle n \rangle$  as well as the normalized second-order correlation function  $g^{(2)}(0)$  as function of scaled detuning  $\Delta/\alpha$ . Here (a,c)  $\Omega/\alpha = 0.06, 0.04, 0.006$  while (b,d)  $\Omega/\alpha = 0.3, 0.2, 0.1$  for the solid, the dashed and the dotted curves, respectively. Other parameters are:  $\gamma/\alpha = 10^{-3}$  and  $2s = 50$ .

excitations, i.e.  $a^\dagger a/2s \ll 1$ , one arrives at the following long-time solution for the normalized diagonal elements  $P_q = \langle q|\rho_s|q\rangle$  of the density matrix  $\rho_s$ :

$$P_q = Z^{-1} \sum_{m=0}^{2s-q} C_{mm} \frac{(q+m)!(2s-q)!}{q!(2s-q-m)!}. \quad (4)$$

Here, the normalization constant  $Z$  is given by the expression:

$$Z = \sum_{m=0}^{2s} C_{mm} \frac{(2s+m+1)!(m!)^2}{(2s-m)!(2m+1)!}, \quad (5)$$

where  $C_{mm} = |\sigma|^{-2m} |\Gamma(1+m+i\phi^*)/[m!\Gamma(1+i\phi^*)]|^2$  and  $\sigma = \Omega/(\gamma \pm i\alpha)$ ,  $\phi = \pm(2s\alpha \pm \Delta)/(\gamma \pm i\alpha)$ , while  $\Omega = \epsilon/\sqrt{2s}$  and  $\gamma = \kappa/2s$ . With the help of the steady-state solution (4), one can calculate the oscillator's variables of interest. In particular, the mean number of excitations in the system  $\langle n \rangle \equiv \langle a^\dagger a \rangle$  as well as its second-order correlation function  $G^{(2)}(0) \equiv \langle a^{\dagger 2} a^2 \rangle$  can be obtained from the following expressions:

$$\langle n \rangle = \sum_{q=0}^{2s} q P_q, \quad G^{(2)}(0) = \sum_{q=0}^{2s} q(q-1) P_q. \quad (6)$$

Because we considered the weak excitation limit, the solution (4) is valid as long as  $\Omega \ll \alpha$ . This means that the amplitude of the external driving  $\epsilon$  should be less or of the order of boson-boson potential  $\alpha$ . Thus, our approach is well suitable to describe low-photon processes with mean-photon numbers of the order of few photons.

We further focus on investigating the properties of the driven and damped non-linear oscillator using Eqs. (4-6).

As a first result, Fig. (1) shows the steady-state dependence of the mean photon number  $\langle n \rangle$  and the normalized second-order correlation function  $g^{(2)}(0) = G^{(2)}(0)/\langle n \rangle^2$  versus the external field detuning  $\Delta/\alpha$  for the negative sign in Eq. (1). There, (a,c) describe the weak field limit whereas (b,d) depict pumping with a moderate coherent source. Interestingly, single-photon light with sub-Poissonian photon statistics can be obtained (see Fig. 1(a,c) near  $\Delta/\alpha = -1$ ). This is not trivial since even weaker fields lead to super-Poissonian photon statistics (see Fig. 1(a,c) at  $\Delta/\alpha < -1$ ). However, the two-photon correlator  $G^{(2)}(0)$  has small values here and larger values for  $g^{(2)}(0)$  are due to even smaller denominator, i.e.,  $\langle n \rangle^2$ . For stronger driving, super-Poissonian photon statistics almost always occurs for  $\Delta/\alpha < -1.5$  and Poissonian or sub-Poissonian statistics for  $\Delta/\alpha > -1.5$  (see Fig. 1(b,d)). Furthermore, the mean photon number shows strong asymmetrical behaviors. The asymmetry is more pronounced for intenser external fields (compare Fig. 1(a) and Fig. 1(b)). Notably, the multi-peak behaviors of the mean photon number can help us to determine the non-linearity  $\alpha$ . One can observe that the scaled frequency interval between the neighbour peaks in Fig. 1(a,b) equals unity and, thus, the corresponding inter-peak frequency will be equal to the non-linearity  $\alpha$ . Therefore, the boson-boson non-linearity can be extracted by measuring the mean photon number against the external pumping field detuning. The only condition is that the non-linearity  $\alpha$  should be at least few times larger than the damping of the quantized mode  $\kappa$ . This is well-satisfied in a wide range of systems [19]. Note that the peaks at  $\Delta/\alpha = -6$  in Fig. (1b) and Fig. (1d) are slightly smaller than those obtained numerically. The inter-peaks interval is obtained correctly for even stronger pumping, however, the magnitude of the peaks as well as their positions will be given only approximately. The same results occur for the positive sign in Eq. (1), i.e., for repulsive boson-boson interactions, though the corresponding curves in Fig. (1) will be mirrored with respect to the  $0Y$  axis. Therefore, for simplicity, we shall consider further only attractive boson-boson interactions.

An explanation of the multi-peak behaviors in Fig. (1) can be found by representing the Eq. (2) via the number state basis, i.e.  $P_{mn} = \langle m | \rho_s | n \rangle$ . Then, for the negative sign in Eq. (1), one arrives at the following terms next to  $P_{mn}$ , that is,  $P_{mn}[i(m-n)\{\Delta + \alpha(m+n-1)\} - \kappa(m+n)]$ . One can observe here that resonances occur at  $\Delta + \alpha(m+n-1) = 0$ , when  $\alpha > \kappa$ . The off-diagonal elements induced by the driving field in the steady-state play a crucial role here. In their absence the mean photon number, for instance, would be insensitive on photon-photon interactions. In a recent work [33], additional resonances were found which may help to extract the non-linear parameters, though in a more complicated setup.

To further describe our system, we plot in Fig. (2)

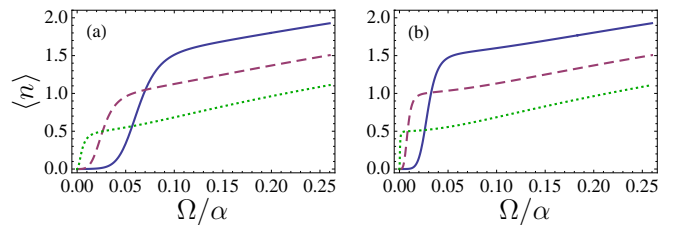


FIG. 2: (color online) The mean photon number  $\langle n \rangle$  versus the intensity of the pumping field  $\Omega/\alpha$ . Solid line is for  $\Delta/\alpha = -2$ , dashed curve corresponds to  $\Delta/\alpha = -1$  while the dotted line to  $\Delta/\alpha = 0$ . Here, (a)  $\gamma/\alpha = 10^{-3}$  and (b)  $\gamma/\alpha = 10^{-4}$  with  $2s = 50$ .

the dependence of the non-linear oscillator's mean photon number as function of the applied field intensity. The detunings are adjusted to values giving the peaks in Fig. (1a). Switching with less than one photon is observed here (see the dotted line in Fig. 2). The mean photon number abruptly increases as the pumping strength varies only a little. For instance, the transition among states with  $\langle n \rangle = 0$  to  $\langle n \rangle \approx 1$  occurs while the intensity of the external pumping field changes between  $\Omega/\alpha \approx 0.005$  and  $\Omega/\alpha \approx 0.02$  (see the dashed curve in Fig. 2b). The switching phenomenon considerably improves for larger boson-boson interactions (compare Fig. 2a and Fig. 2b). Positive values of  $\Delta$ , away from resonance, do not lead to switching effects. These critical behaviors take place for repulsive photon-photon interactions too, but for  $\Delta \geq 0$ . Thus, the appropriately prepared non-linear sample can be presented as a single-photon optical switching device. Finally, for comparison, we have obtained the oscillator's mean photon number and its second-order correlation function without taking into account of the boson-boson interaction potential, i.e., we set  $\alpha = 0$ :

$$\langle n \rangle = \frac{\epsilon^2}{\kappa^2 + \Delta^2}, \quad G^{(2)}(0) = \frac{\epsilon^4}{(\kappa^2 + \Delta^2)^2}. \quad (7)$$

In this case, however, the rich variety of effects shown in Fig. (1) and Fig. (2) vanishes and the photon statistics always shows Poissonian photon distribution.

In the experiment described in Ref. [15], few-photon switching, Kerr non-linearity and dispersive optical bistability of a Fabry-Perot optical resonator due to the displacement of ultracold atoms trapped within were reported. There, the photon asymmetry similar to the one shown in Fig. 1(a,b) was observed as well (see also Fig. 2 in [15]). Though experimentally, they got multiple peaks of the intracavity mean photon number their nature was not explained. Based on our results, we can conjecture that the interval between the main peaks around the central one of the intracavity mean photon number obtained in [15] may give the induced boson-boson non-linearity. Optical switching with single photons was observed as well [34].

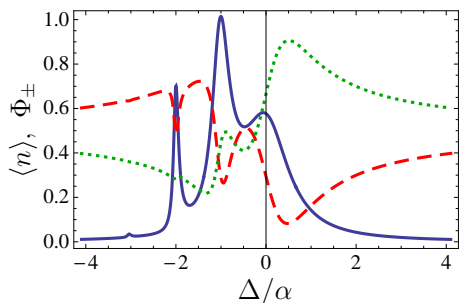


FIG. 3: (color online) The mean photon number  $\langle n \rangle$  as well as the fidelities  $\Phi_{\pm}$  against the pumping field detuning  $\Delta/\alpha$ . The solid line depicts the mean photon number  $\langle n \rangle$  while the dashed and the dotted curves correspond to  $\Phi_{-}$  and  $\Phi_{+}$ , respectively. Here,  $\Omega/\alpha = 0.06$ ,  $\gamma/\alpha = 10^{-3}$  and  $2s = 50$ .

In order to look at more details in the few-photon processes emphasized here, in Fig. (3), we plot the fidelities  $\Phi_{\pm} = \langle \Psi_{\pm} | \rho_s | \Psi_{\pm} \rangle$  of entangled states

$$|\Psi_{\pm}\rangle = \frac{1}{\sqrt{2}}(|0\rangle \pm |1\rangle), \quad (8)$$

where  $|0\rangle$  and  $|1\rangle$  are the number state basis with zero and one photon, respectively. There, the dashed curve corresponds to  $\Phi_{-}$  while the dotted one to  $\Phi_{+}$ . The solid line shows the non-linear oscillator's mean photon number  $\langle n \rangle$ . The parameters are the same as for the solid line in Fig. (1a). One can observe here that at  $\Delta/\alpha = 0.5$  the entangled state  $|\Psi_{+}\rangle = (|0\rangle + |1\rangle)/\sqrt{2}$  is created with a fidelity  $\Phi_{+} \approx 0.9$  and  $\langle n \rangle \approx 0.4$ , while the photon statistics is sub-Poissonian (see Fig. 1c). On the other side, at  $\Delta/\alpha = -1.5$  the entangled state  $|\Psi_{-}\rangle = (|0\rangle - |1\rangle)/\sqrt{2}$  occurs with a fidelity  $\Phi_{-} \approx 0.7$  and  $\langle n \rangle \approx 0.2$ , and where photon statistics is super-Poissonian (see Fig. 1c). Larger fidelities mean establishing of quantum coherences in the system and, thus, proving the quantum nature of the states (8). Note that for detunings approximately within  $-2.1 < \Delta/\alpha < 0$  one has  $\Phi_{+} + \Phi_{-} < 1$  denoting the existence of higher Fock states, i.e.  $|n > 1\rangle$ , though with smaller probabilities (see Fig. 3). Therefore, we have demonstrated here switching and entanglement with less than one photon processes.

In summary, we have shown how to measure the photon-photon interaction potential via weakly pumping the quantized mode with which the examined system interacts. The non-linear effect induces multiple peaks in the mean photon number steady-state behaviors with inter-peaks intervals equating the required non-linearity. For this to occur the boson-boson non-linearity should be larger than the quantized mode damping. This requirement is well-fulfilled in a wide range of systems. Due to the involved non-linearity, an asymmetry in the first- and second-order field correlation functions was observed as well. In addition, we have demonstrated switching and high-fidelity entanglement with less than one photon pro-

cess. Sub-Poissonian photon statistics occurs for particular external controllable parameters. The reported results can be tested with existing experiments.

\* Electronic address: mihai.macovei@mpi-hd.mpg.de

- [1] P. D. Drummond, D. F. Walls, J. Phys. A: Math. Gen. **13**, 725 (1980).
- [2] A. Imamoglu *et al.*, Phys. Rev. Lett. **79**, 1467 (1997).
- [3] M. D. Lukin, A. Imamoglu, Phys. Rev. Lett. **84**, 1419 (2000); B. S. Ham, P. R. Hemmer, Phys. Rev. Lett. **84**, 4080 (2000).
- [4] H. Schmidt, A. Imamoglu, Opt. Lett. **21**, 1936 (1996).
- [5] H. Wang, D. Goorskey, M. Xiao, Phys. Rev. Lett. **87**, 073601 (2001).
- [6] Y. Niu, S. Gong, Phys. Rev. A **73**, 053811 (2006).
- [7] R. Tan, G.-x. Li, Z. Ficek, J. Phys. B: At. Mol. Opt. Phys. **42**, 055507 (2009).
- [8] T. N. Dey, G. S. Agarwal, Phys. Rev. A **76**, 015802 (2007).
- [9] H. Michinel, M. Paz-Alonso, V. Perez-Garcia, Phys. Rev. Lett. **96**, 023903 (2006).
- [10] K. Dolgaleva, H. Shin, R. Boyd, Phys. Rev. Lett. **103**, 113902 (2009).
- [11] G. Y. Kryuchkyan, S. B. Manvelyan, Phys. Rev. Lett. **88**, 094101 (2002); P. Bardetski, N. Enaki, D. Mihalache, JETP **83**, 653 (1996).
- [12] Ch. Silberhorn *et al.*, Phys. Rev. Lett. **86**, 4267 (2001).
- [13] L. Hau *et al.*, Nature (London) **397**, 594 (1999).
- [14] H. Kang, Y. Zhu, Phys. Rev. Lett. **91**, 093601 (2003).
- [15] S. Gupta *et al.*, Phys. Rev. Lett. **99**, 213601 (2007).
- [16] M. Vengalattore *et al.*, Phys. Rev. Lett. **101**, 063901 (2008).
- [17] K. M. Birnbaum *et al.*, Nature (London) **436**, 87 (2005).
- [18] K. Jacobs, A. Landahl, Phys. Rev. Lett. **103**, 067201 (2009).
- [19] S. Rebic, J. Twamley, G. Milburn, Phys. Rev. Lett. **103**, 150503 (2009).
- [20] S. A. Moskalenko and D. W. Snoke, *Bose-Einstein Condensation of Excitons and Biexcitons and Coherent Nonlinear Optics with Excitons*, (Cambridge University Press, Cambridge, UK, 2000).
- [21] G. S. Agarwal, Phys. Rev. A **51**, R2711 (1995).
- [22] A. Verger, C. Ciuti, I. Carusotto, Phys. Rev. B **73**, 193306 (2006).
- [23] I. Katz *et al.*, Phys. Rev. Lett. **99**, 040404 (2007).
- [24] M. Marthaler, G. Schön, A. Shnirman, Phys. Rev. Lett. **101**, 147001 (2008).
- [25] D. H. Santamore *et al.*, Phys. Rev. A **70**, 052105 (2004).
- [26] I. Serban, F. Wilhelm, Phys. Rev. Lett. **99**, 137001 (2007).
- [27] H. Nakano *et al.*, Phys. Rev. Lett. **102**, 257003 (2009).
- [28] H. Ge, H. Qian, Phys. Rev. Lett. **103**, 148103 (2009).
- [29] H. J. Carmichael, *An Open Systems Approach to Quantum Optics*, (Springer, Berlin, 1993).
- [30] D. F. Walls, G. J. Milburn, *Quantum Optics*, (Springer, Berlin, 1994).
- [31] T. Holstein, H. Primakoff, Phys. Rev. **58**, 1098 (1940).
- [32] S. Ya. Kilin, Sov. Phys. JETP **55**, 38 (1982).
- [33] I. Carusotto *et al.*, Phys. Rev. Lett. **103**, 033601 (2009).
- [34] B. Dayan *et al.*, Science **319**, 1062 (2008).